Available online at www.sciencedirect.com
SCIENCE DIRECT®
Journal of Power Sources 143 (2005) 197–202
JOURNAL OF POWER SOURCES
www.elsevier.com/locate/jpowsour

Electrochemical impedance study of graphite/electrolyte interface formed in LiBOB/PC electrolyte

Kang Xu*, Shengshui Zhang, Richard Jow

Army Research Laboratory, Sensor and Electron Device Directorate, Adelphi, MD 20783-1197, USA

Received 27 September 2004; accepted 4 November 2004
Available online 15 January 2005

Abstract

Electrochemical impedance measurements were performed on graphitic anodes during their galvanostatic cycling in LiBOB/PC electrolyte, and the variation of each impedance component was studied as the function of the lithiation state. It was found that the charge-transfer component was closely related to the formation of the solid electrolyte interface (SEI), characterized by a sharp drop in the corresponding resistances between OCV and 0.60 V, while the semi-circle in the medium frequency range might arise from contact impedance components within the electrode, because it varies reversibly during the lithiation/delithiation cycle.

The irreversible reduction process at 1.70 V, which is characteristic of LiBOB salt, was confirmed to originate from the reductive decomposition of oxalate ester impurities, and this process is believed to be unrelated to the protective SEI formed by LiBOB electrolytes on graphitic anode. When compared with the corresponding $LiPF_6$-based electrolytes, it was concluded that the alkyl carbonates are not appropriate solvents for LiBOB salt, both in terms of the power and low temperature performances in lithium ion cells.
Published by Elsevier B.V.

Keywords: LiBOB electrolytes; Electrochemical impedance; Graphite/electrolyte interface

1. Introduction

A borate-based new salt, lithium bis(oxalato)borate (LiBOB), was recently proposed as a possible alternative for the thermally unstable $LiPF_6$ as electrolyte solute in lithium ion battery [1,2]. The main advantage of this new salt was highlighted by the relatively stable cycling performance of the electrolytes based on it in lithium ion cells at elevated temperatures [3]. In the follow up studies a unique property of this new salt in forming an effective solid electrolyte interface (SEI) on graphitic anode was also reported [4], and the possible potential range within which this protective interface was formed was placed below 1.0 V [5]. Surface analysis of the formed graphitic anode surface revealed that the SEI formed in LiBOB-electrolyte is very similar in chemical nature to that formed in $LiPF_6$-based electrolytes, i.e., semi-carbonate species serve as the key ingredients in protecting the graphitic structure. The major difference lying between the LiBOB- and the $LiPF_6$-originated SEI is the content of these semi-carbonate species, which was at low percentage versus the pristine carbon signal in the latter (∼5%) but sharply higher in the LiBOB-originated SEI (∼30%) [6]. Preliminary conclusions were drawn that the salt anion, which is rich in carbonyl species, plays an active role in dictating the chemical nature of the SEI, and that the high temperature stability of the electrolytes based on LiBOB very likely arises from this new SEI with enriched semi-carbonate species as a result of the anion-participation.

To better understand this new surface chemistry between LiBOB-electrolyte and graphitic anode, we carried out the electrochemical impedance spectra (EIS) measurement on the graphitic anodes in LiBOB/PC electrolyte during their lithiation/delithiation cycles, and established a correlation between the potential-dependences of SEI formation and the cell impedance components. This correlation would help to

* Corresponding author. Tel.: +1 301 394 0043; fax: +1 301 394 0273.
E-mail address: cxu@arl.army.mil (K. Xu).

0378-7753/$ – see front matter. Published by Elsevier B.V.
doi:10.1016/j.jpowsour.2004.11.026

depict a dynamic picture of the forming process of the BOB-originated SEI, in combination with other electrochemical and spectroscopic techniques we have adopted.

On the other hand, despite the favorable interfacial and thermal properties that LiBOB has shown, the bulk properties of this new salt in alkyl carbonate solvents, such as solubility and ion conductivity, have been found to be inferior to those of $LiPF_6$, and concerns have been raised regarding the practical use of LiBOB in lithium ion cells. With EIS study of lithium ion cells containing LiBOB in carbonate solutions, we hope to determine whether the above bulk transport properties are reflected in the interfacial charge-transfer processes and thus affect the cell power capabilities. This paper summarizes part of the EIS work performed in our lab.

2. Experimental

LiBOB was synthesized in our lab through an aqueous approach as described in a patent disclosure [1]. Repeated recrystallization in appropriate solvents yields this salt of high purity (>99% by ^{11}B-NMR and >99.5% by Li-content determination with atomic absorption spectroscopy). Propylene carbonate (PC), ethylmethyl carbonate (EMC), ethylene carbonate (EC) from EM Sciences (>99.99%) and diethyl oxalate (DEO) from Aldrich (99%) were dried over neutral alumina, and the moisture level as determined by Karl–Fischer titration was ~6.00 ppm or lower. The electrolyte solutions were prepared in a Vacuum Atmosphere glove box with oxygen and moisture levels below 10 and 5 ppm, respectively. An 1.0 m $LiPF_6$ in EC/EMC was used as the baseline electrolyte, with DEO as the model impurity at concentration levels of 1, 5 and 10%, respectively. Graphitic anode composites coated on Cu foil were provided by SAFT. These electrode sheets were cut into discs of area 1.27 cm^2.

Button cells of size 2335 served as testing vehicles for half cells in galvanostatic cycling as well as impedance studies. Since the design and the configuration of the anode half cell is of critical importance to the reproducibility of the impedance measurements, the detailed parts of the button cells used in this study are shown in Fig. 1. The cell cases and lids (Rayovac) were made of Type 223 stainless steel, while the spacers and the springs were from Hohsen Corp., Japan. The assembly was crimped using a Rayovac Multipress in a dry-room with dew point of ca. −60 to −70 °C. Before each impedance test the cells were cycled to a specified potential galvanostatically at the rate of 0.093 mA cm^{-2} by a Solartron SI 1287 Electrochemical Interface. The ac impedance measurement was then conducted on such cells by using a Solartron SI 1260 Impedance/Gain-Phase Analyzer. A dc bias equivalent to the cell potential was applied to the cell, while an ac perturbation of 0.10 mV in amplitude was generated in the frequency range of 0.01–10^6 Hz. In this way the impedance spectra measured would describe the interface of the electrode at the known state of charge. Both the cycling and impedance testing were controlled by CorrWare and Zplot softwares, while the collected data were fitted and analyzed by the corresponding softwares CorrView and ZView.

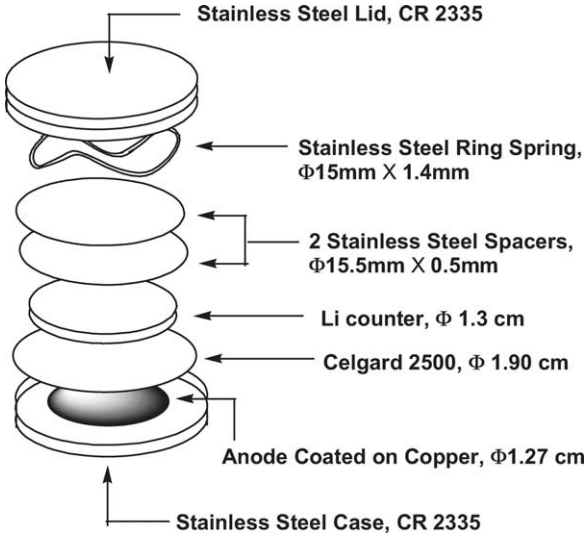

Fig. 1. Exploded view of the anode half cell used in the electrochemical impedance study.

3. Results and discussion

3.1. Measurement and fitting of EIS

In Fig. 2 the typical impedance response recorded in the Li/graphite half cell is shown and is composed of two depressed semi-circles in the high and medium frequency ranges and a short spike in the low frequency range. It has been generally accepted that the semi-circle in the medium frequency range arises from the impedance of the, interfacial film on the electrode, while the one in the lower frequency range arises from the charge-transfer process [7,9]. The spike at the low frequency end indicates the long range ion

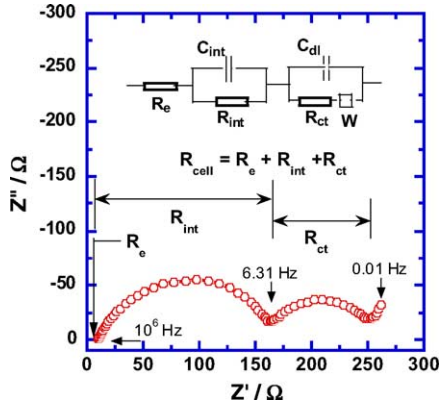

Fig. 2. The complex plane (Nyquist plots) of Li/LiBOB in PC/graphite cell at the cell potential of 0.05 V during discharging (lithiation). Selected frequencies are indicated in the figure. Inset: the equivalent circuit used to fit the impedance data.

diffusion in the bulk of the graphite, and its angle with the real axis changes with cell potential from 90° progressively to 45°, which is typical of semi-infinite diffusion. An equivalent circuit with individual components as shown in the inset of Fig. 2 was used to fit the EIS data, where the above processes were represented by two RC subsets in series, with the corresponding resistances R_{int} (interfacial) and R_{ct} (charge-transfer). The total cell resistance R_{cell} is then defined as the summation of R_{int} and R_{ct} plus an ohmic component (R_e), which reflects the summation of bulk ionic conductivity of the electrolyte, electronic conductivity in bulk graphite, and the contact resistance between electrode coating and substrate. In practical applications it is R_{cell} that is of significance because the ion transport across the cell, or the cell power performance, is directly dictated by it.

It should be pointed out that the good reproducibility of any EIS experiment lies in the reliable resolution of these different impedance responses. More specifically, it would be difficult to obtain reliable data for individual components R_{int} and R_{ct} if the two semi-circles had been merged due to similar time constants, because arbitrariness has to be involved to fit such data to the equivalent circuit. Unfortunately, this situation occurs more often than not, especially at low cell potentials where the graphite is nearly fully lithiated, and the semi-circle corresponding to charge-transfer appears as a vanishing shoulder of the larger interfacial component [7,10]. On the other hand, we found that by adopting the cell design shown in Fig. 1, the time constants for these two semi-circles could be distinctively separated in most of the entire potential range studied, as shown by the example in Fig. 2 which was measured at 0.05 V. The two processes (R_{int} and R_{ct}) also remains well separated for most of the electrolyte systems we investigated.

As we have reported earlier, the total cell impedance of Li/graphite half cell based on the state-of-the-art electrolytes ($LiPF_6$- and EC-based) is dominated by two components, i.e., R_{int} and R_{ct} [9], and both components change drastically with the cell potential, because the lithiation state of the graphite anode dictates the lithium ion diffusion through the SEI and into the bulk graphene structure. Of special interest was the potential range where the main stage in formation of an effective SEI is thought to occur (~0.20 V), which is characterized by a steep drop in the interfacial impedance of the cell. Apparently the electrode surface undergoes substantial change at this specific potential due to the deposition from electrolyte reduction, although we are still unsure if an effective SEI is indeed completed at this stage. On the other hand, the unique property of LiBOB in neat PC solution has enabled us to accurately determine the completion of such an effective SEI, i.e., we have observed that only when a graphite anode was preformed in LiBOB/PC down to 0.55 V or lower potentials can it support the reversible lithium intercalation/de-intercalation in $LiPF_6$/PC. The latter electrolyte composition has been well known to exfoliate the graphite structure [5].

To find if a similar correlation between R_{int} and SEI formation exists in LiBOB/PC, we cycled graphitic anodes from

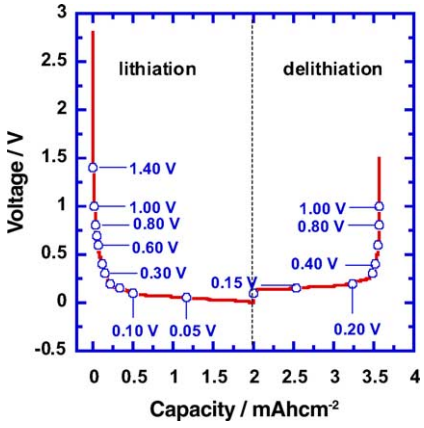

Fig. 3. The galvanostatic cycling of graphitic anode in LiBOB/PC. Only the first cycle is shown. Electrochemical impedance spectra were measured during both discharge (lithiation or cathodic polarization) and charge (delithiation or anodic polarization) processes at the indicated spots.

the open circuit voltage (OCV, ~3.0 V) down to 0.050 V in LiBOB/PC, while interrupting the cycling to conduct a series of EIS measurements at pre-selected potentials. These potentials at which EIS study were carried out are marked in Fig. 3 on the voltage-capacity profile of such a half cell. The spectra thus generated were fitted to the equivalent circuit as shown in the inset of Fig. 2, and the dependences of the resistances for each individual component are plotted in Fig. 4 for comparison. Due to the vast difference in the scales of these data sets, R_e and R_{int} are plotted together (Fig. 4a), and so are R_{ct} and R_{cell} (Fig. 4c), respectively. For clarity, Fig. 4 (and also Figs. 5 and 6) was plotted in such a way that the data points for discharge (lithiation) and charge (delithiation) processes are separated along the horizontal axis, so that overlapping between these two processes due to similar data values is avoided. Thus, the left halves of these figures represent the initial lithiation (charge) process of the graphite anode, while the right halves reflect the delithiation process of the same anode with an already-formed SEI (Fig. 4b).

3.2. Dependence of R_e and R_{int} on cell potential

During the whole potential range tested (lithiated from 3.0 V down to 0.05 V then delithiated back to 1.0 V), resistance of the ohmic component R_e experiences little variation, which is understandable because the bulk ion conductivity and electric contact resistance etc are hardly affected by the electrochemical states of the graphite anode. Meanwhile, R_{int} representing interfacial film component starts a gradual drop between 1.7 and 1.0 V, approximately corresponding to an irreversible process previously observed during galvanostatic cycling (inset, Fig. 4b) [5]. This process is characteristic of LiBOB-containing electrolytes, and through the synthesis and testing of LiBOB we have suspected that this irreversible process is probably caused by trace impurity in the salt.

Since LiBOB in our work was synthesized from oxalic acid and boric acid, a likely source of impurity is the unreacted

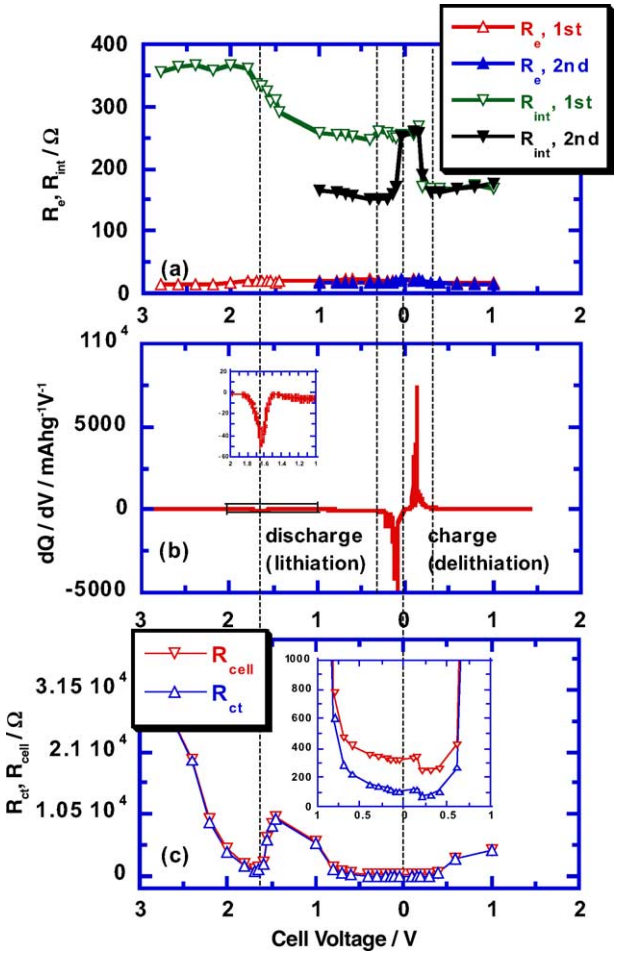

Fig. 4. The dependence of the cell resistance on anode potential: (a) ohmic and interfacial components for the first and the second cycles; (c) charge-transfer component and the summation of resistance components of the cell for the first cycle. The potential-dependence of differential capacity for the anode in the first cycle is also shown (b) to demonstrate the correlation between various electrochemical processes and these impedance components.

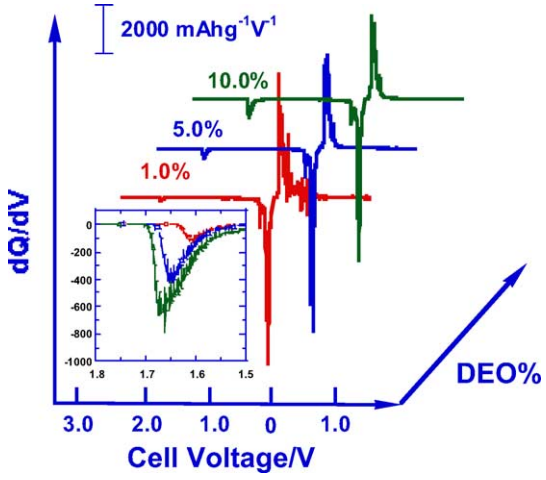

Fig. 5. The effect of oxalate impurity on the potential-dependence of differential capacity. The baseline electrolyte is 1.0 M $LiPF_6$ in EC/EMC (1:1 by weight). Note that the irreversible capacity for the process at 1.70 V increases monotonically with DEO content.

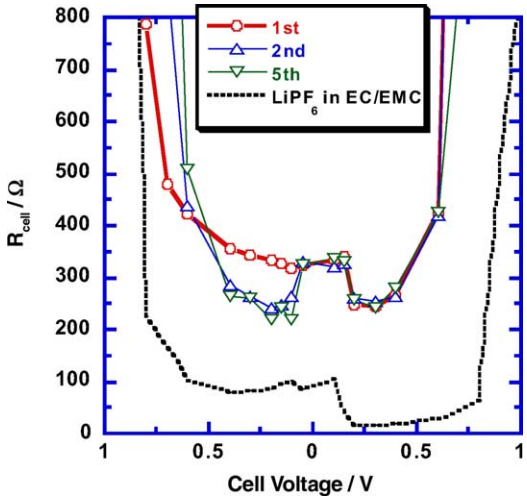

Fig. 6. The potential dependences of cell impedance in the first five cycles (only the first, second and fifth shown). The cell impedance for $LiPF_6$/EC/EMC during the first lithiation cycle was included as benchmark.

or partially reacted oxalic salt or ester. Based on this inference, we have previously assigned the above 1.7 V process to the reduction of oxalic salt or ester [5]. In order to further confirm this identity, we use a dialkyl ester of oxalic acid, DEO, as a model compound and deliberately added it as an impurity into a baseline electrolyte (1.0 m $LiPF_6$/EC/EMC), which does not have any detectable process near 1.7 V. Fig. 5 shows the differential capacity versus voltage for the Li/graphite cells based on these "contaminated" electrolytes with DEO concentrations at 1, 5 and 10%, respectively. In all electrolytes, the 1.7 V process is reproduced, and the peak intensity increases monotonically with impurity level.[1] Thus we tentatively conclude that this 1.7 V process is caused by impurity existing in the salt, and the corresponding drop in R_{int} might not reflect the formation of an effective SEI.

Surprisingly, between 0.60 and 0.55 V there is no apparent change in R_{int}, although we have determined that this is the potential range where SEI is completed [5]. Considering the essential change in the chemical nature of the surface during the above potential range, i.e., the surface turns from being vulnerable to PC-cointercalation to being able to stably support reversible lithium ion intercalation, a direct correlation is hard to establish between R_{int} and the formation of SEI. Similar result has been observed in different systems for R_{int} [8], suggesting that this component at the medium frequency range might not be actually associated with the SEI as its nominal assignment would hint. Considering the phenomenological nature of the EIS technique, the above "inconsistence" should not be surprising. Actually, there has been a proposition that this semi-circle of R_{int} is more related to the contact resistance between the paste of active mate-

[1] A rough estimate of impurity level for the LiBOB salt used in this study could be made based on the comparison of the irreversible capacities at 1.7 V (between Fig. 4b and Fig. 5), which should be less than 0.6% and agrees well with AAS analysis result [5].

rial and the current collector [8]. Similarly, we believe that it is more likely related to the intergrain resistance within the anode, as its variation with cell potential coincides with the repeated expansion/contraction cycle of the latter as we will see in the subsequent cycles following the initial formation cycle (Fig. 4a and Fig. 6).

In Fig. 4a, after the drop at 1.7 V, R_{int} stabilizes through the entire lithiation process, and while the cell starts to delithiate, it drops abruptly to a low level (∼150 Ω). Repeated tests on multiple cells reproduced the above abrupt drop in R_{int}, as did the tests conducted on the following cycles. In Fig. 4a test results for R_e and R_{int} during the second cycle are also shown as an example. While no notable change in the potential-dependence of R_e can be detected, the value of R_{int} at the beginning of the second lithiation starts at the same low level (∼150 Ω) with that at the end of the first delithiation. In a narrow potential range between 0.20 and 0.01 V, R_{int} rises and forms an elevated platform with a height of 260 Ω. The abrupt drop occurs again at ∼0.20 V during charge and forms the end of the elevation, and values of R_{int} almost perfectly coincide with those in the first delithiation process. The same potential-dependence was obtained for R_{int} during all the subsequent cycles with good reproducibility, which is not shown in Fig. 4a for graphic simplicity. In other words, R_{int} reversibly increases to a constant value at potentials below 0.20 V, when the graphene structure is lithiated. The total cell resistance R_{cell} will be affected by this peculiar potential-dependence within this potential range.

3.3. Dependence of R_{ct} and R_{cell} on cell potential

Unlike R_e and R_{int}, R_{ct} decreases rapidly during the first lithiation process, and arrives at a minimum at ca. 1.65 V, which coincides well with the irreversible process discussed above. The correlation between this process and R_{int}/R_{ct} does not seem to be accidental, but rather demonstrates that the reduction of the impurity might result in some form of deposition on the graphite surface, although this deposition is still not sufficient to function as protective film against PC-cointercalation and graphene exfoliation. According to our previous report on state-of-the-art electrolyte, R_{ct} usually arrives at minimum values when there is a phase change within the anode involved [9]. Therefore, we speculate that the possibility for oxalic salt or esters to be irreversibly cointercalated into graphene layers at 1.7 V cannot be excluded.

On the other hand, an obvious variation between 1.0 and 0.50 V occurs in the resistance of the charge-transfer process R_{ct} (Fig. 4c and its inset), which drops from ∼5000 Ω at 1.0 V to ∼200 Ω at 0.60 V. Below 0.60 V the drop continues but at a much slower rate, and R_{ct} stabilizes between 150 and 110 Ω in the potential range of 0.50 and 0.01 V. This drastic drop in R_{ct} between 1.0 and 0.60 V, before the lithium ion intercalation happens, should correspond with the formation process of the SEI since we know that effective protection against PC cointercalation is completed at this potential [5]. After the lithiation was completed, the graphitic anode was then subjected to delithiation, and R_{ct} shows a similar potential dependence to that of R_{int}, i.e., a drop occurs at ∼0.20 V.

Also plotted in Fig. 4c is the dependence of total cell resistance R_{cell} on cell potential. Apparently, this dependence is dominated by the contribution from R_{ct}.

In a full lithium ion cell, the potential of the graphitic the anode after the initial formation cycles can vary between 0.80 and 0.01 V during normal operation. In other words, according to the results shown in Fig. 4c, after the formation of the SEI, the resistance to the lithium ion charge-transfer process (and hence the cell resistance R_{cell}) stays at a low level (<300 Ω for graphite in LiBOB/PC), thus allowing the operation of lithium ion chemistry to occur reversibly and with low polarization. This conclusion is drawn from our previous report [9] and is further supported by the extended EIS studies on the graphitic anode in the subsequent cycles shown in Fig. 6, where only the results of R_{cell} for second and fifth cycle are selected for clarity, while the result for the first cycle is also included for comparison. Noticeably, in the formed cell the resistance R_{cell} stays at a much lower level compared to the cell during formation. Actually, from the second lithiation process on, the dependence of R_{cell} appears as a mirror image to that of the R_{cell} during the first delithiation process, instead of tracking the dependence of R_{cell} during the first lithiation process. This potential dependence will hold true for all the subsequent cycles, and as a result the plots of R_{cell} versus cell potential for these cycles take a symmetrical shape as shown in Fig. 6, in sharp contrast to the asymmetrical shape for the initial cycle. This new constancy achieved in the dependences of R_{cell} on cell potential indicates the stability of the graphitic anode surface after an effective SEI is formed.

Another very interesting note to make is that the R_{cell} value oscillates reversibly between ∼250 and ∼350 Ω in a narrow potential range of 0.20–0.01 V, during both lithiation and delithiation processes. This excursion in R_{cell} value forms an elevated platform in its symmetrical potential dependence (Fig. 6) for all the following cycles after the first forming cycle, apparently due to the contribution from both R_{ct} and R_{int} (see Fig. 4a and c). A closer examination reveals that the potential range within which this platform is located corresponds well with that of the main lithiation/delithiation reactions of the graphitic anode, as shown by the potential dependence of differential capacity of the graphitic anode in LiBOB/PC plotted in Fig. 4b.

The three distinctive lithiation processes in Fig. 4b at ∼0.20, ∼0.12 and ∼0.09 V were the well-known phase transitions between the graphite intercalation compounds at stage 1 to 4, stage 2L to 2, and stage 2 to 1, respectively [7,11]. In other words, these higher values of R_{int} coincide with the existence of a graphene structure fully loaded with lithium ions. This correlation seems to be a support for the earlier suggestion made by Chang and Sohn [8] that the semi-circle in the medium frequency range is related to contact impedance factors within the electrode rather than the surface film, because the mechanical stress introduced by the expanded graphene interlayer distance in a fully loaded anode

is likely to be associated with increased contact impedances, either inter-grain (as we believe) or between active mass and substrate (as suggested by Chang and Sohn) [8].

Finally, some comments should be made on the practical applicability of LiBOB-based electrolytes in lithium ion batteries, considering its lower conductivity/solubility in alkyl carbonate solvents. A rough comparison is made between LiBOB/PC and state-of-the-art electrolyte for the lithium ion battery in terms of cell impedances in graphitic anode half cells. The potential-dependence of R_{cell} for $LiPF_6$ in EC/EMC (1:1 by weight) was plotted in Fig. 6, and similar to that of the LiBOB/PC electrolyte, the cell impedance stabilized after SEI formation. However, when compared with LiBOB/PC, the resistance of $LiPF_6$-based electrolytes remained at a much lower level ($\sim$20 Ω) after the formation of its SEI. Although with the addition of the less viscous linear carbonates such as DMC, EMC or DEC, the LiBOB-based electrolytes can achieve higher ion conductivity and lower impedance levels, the difficulty still exists for it to be competitive with the electrolytes based on $LiPF_6$ in terms of power performance. Based on our experience with this new salt, it seems that the alkyl carbonates, which are the current commonly used solvents in the lithium ion battery industry, are not the most suitable solvents for LiBOB if power performance or low temperature performance is the focus. In order for LiBOB to replace $LiPF_6$ as an electrolyte solute for the above purpose, new solvent systems in which LiBOB has high solubility and high ion conductivity have to be sought. Certainly, if the application is restricted to an elevated temperature range, then the above disadvantages are no longer so pronounced, and LiBOB in alkyl carbonate solutions remains an electrolyte of choice.

4. Conclusion

EIS studies were carried out systematically on graphitic anodes cycling in LiBOB/PC electrolytes at potentials of interest, and the potential-dependence of various impedance components was derived. It was found that the impedance responses represented by the semi-circle at medium frequency range might not have direct relation to the formation of an SEI, while the charge-transfer component shows significant change within the potential range where SEI is believed to be formed. An irreversible reduction process at 1.70 V was confirmed to be caused by an impurity less than 0.6% in LiBOB salt, and it does not seem to contribute to the effective SEI formed at potentials down to 0.55 V. Compared with the state-of-the-art electrolytes based on $LiPF_6$, the power and low temperature performance of LiBOB-based electrolytes in lithium ion cells still need improvement, despite their promising high temperature performance.

Acknowledgements

This work is funded by the FreedomCar Program of the U.S. Department of Energy. The authors also want to thank Drs. Kamen Nechev and Guy Chagnon of SAFT America for the graphitic electrodes.

References

[1] U. Lischka, U. Wietelmann, M. Wegner, Ger. DE 19829030 C1 (1999).
[2] W. Xu, C.A. Angell, Electrochem. Solid State Lett. 4 (2001) E1.
[3] K. Xu, S.S. Zhang, T.R. Jow, W. Xu, C.A. Angell, Electrochem. Solid-State Lett. 5 (2002) A26.
[4] K. Xu, S. Zhang, B.A. Poese, T.R. Jow, Electrochem. Solid-State Lett. 5 (2002) A259.
[5] K. Xu, S. Zhang, T.R. Jow, Electrochem. Solid-State Lett. 6 (2003) A117.
[6] K. Xu, U. Lee, S. Zhang, M. Wood, T.R. Jow, Electrochem. Solid-State Lett. 6 (2003) A144.
[7] A. Funabiki, M. Inaba, Z. Ogumi, S. Yuasa, J. Otsuji, A. Tasaka, J. Electrochem. Soc. 145 (1998) 172.
[8] Y. Chang, H. Sohn, J. Electrochem. Soc. 147 (2000) 50.
[9] S. Zhang, M. Ding, K. Xu, J. Allen, R. Jow, Electrochem. Solid-State Lett. 4 (2001) A206.
[10] Y. Chang, J. Jong, G. Fey, J. Electrochem. Soc. 147 (2000) 2033.
[11] J.R. Dahn, Phys. Rev. B 44 (1991) 9170.